

OPINION

Stomatal Parameters in a Changing Environment

Correspondence: Aaron Potkay (potka002@umn.edu)

Received: 22 August 2024 | **Revised:** 4 November 2024 | **Accepted:** 5 November 2024

Funding: This study was supported by National Oceanic and Atmospheric Administration and National Science Foundation.

1 | Introduction

Stomata are small pores on leaves that allow carbon and water to exchange between leaves and the atmosphere. Mathematical representations of stomatal conductance (g_c for CO_2 , g_w for water vapor; $\text{mol m}^{-2} \text{s}^{-1}$) are necessary for describing photosynthetic net carbon assimilation (A_n ; $\text{mol m}^{-2} \text{s}^{-1}$) and transpiration (E ; $\text{mol m}^{-2} \text{s}^{-1}$). Advancing stomatal conductance models is essential for predicting future carbon and water fluxes and plant performance under a changing climate. These models have long taken on an empirical form (Jarvis 1976), typically predicting stomatal behavior from A_n , the atmospheric CO_2 partial pressure (c_a ; mol mol^{-1}), and either the relative humidity (RH) or the vapor pressure deficit (VPD) between the leaf and air (D_L ; kPa), such as in the models of Ball, Woodrow and Berry (1987) and Leuning (1990, 1995). The semi-empirical Unified Stomatal Optimization (USO) model (Equation 1) was derived by Medlyn et al. (2011) as an approximate solution to the classic optimization theory of Cowan and Farquhar (1977), who theorized that stomata open and close to maximize A_n given a finite water supply,

$$g_c = g_0 + \left(1 + \frac{g_1}{\sqrt{D_L}}\right) \frac{A_n}{c_a}, \quad (1)$$

where g_0 and g_1 are intercept ($\text{mol m}^{-2} \text{s}^{-1}$) and slope ($\text{kPa}^{0.5}$) parameters. The USO has since been widely fitted to leaf-level (Lin et al. 2015) and ecosystem-level (Knauer et al. Werner, and Zehle 2015, 2018; Sloan and Feng 2023) data to examine gas exchange and predict stomatal sensitivity to environmental conditions and is used to predict carbon and water fluxes in land surface models (Bonan et al. 2014; De Kauwe et al. 2015; Franks et al. 2017, 2018). Medlyn et al.'s (2011) derivation originally lacked g_0 , but g_0 was added to resemble empirical models (Ball, Woodrow, and Berry 1987; Leuning 1990, 1995), allowing for non-zero conductance when $A_n = 0$. Studies often disregard g_0 (Lin et al. 2015;

Gimeno et al. 2016; Gardner et al. 2023; Stefanski et al. 2023) because estimates of g_0 and g_1 are correlated, and estimated g_0 are either inflated when the model fits poorly to data or often negative (Duursma et al. 2019).

In the absence of both g_0 and boundary layer resistances, the meaning of g_1 may be defined in terms of solely the leaf internal CO_2 partial pressure (c_i ; mol mol^{-1}), D_L , and either c_a or the water-use efficiency (WUE = A_n/E ; mol mol^{-1}), an indicator of plant performance, (Medlyn et al. 2017) as

$$g_1 = \frac{\frac{c_i}{c_a} \sqrt{D_L}}{1 - \frac{c_i}{c_a}} = \frac{c_i}{1.6 \text{WUE} \sqrt{D_L}}. \quad (2)$$

Larger g_1 and smaller WUE cause larger g_c , A_n , and E . Once g_1 is independently estimated (often from gas exchange measurements), g_c , A_n , and E may be predicted by coupling Equation 1 or 2 with equations of gas diffusion and a model of biochemical carbon fixation (e.g., Farquhar, von Caemmerer, and Berry 1980). Combing the solution for c_i , rearranged from Equation 2, with the simplified model of biochemical carbon fixation,

$$A_n = f_0 \frac{c_i - \Gamma^*}{c_i + \gamma} - R_d, \quad (3)$$

where Γ^* is the CO_2 photosynthetic compensation point (mol mol^{-1}), R_d is the respiration rate ($\text{mol m}^{-2} \text{s}^{-1}$), and f_0 ($\text{mol m}^{-2} \text{s}^{-1}$) and γ (mol mol^{-1}) are parameters, and standard gas diffusion equations (assuming negligible boundary layer and mesophyll resistances) gives the following solutions for A_n , g_c , E , and WUE,

$$A_n = f_0 \frac{c_a g_1 - (g_1 + \sqrt{D_L}) \Gamma^*}{c_a g_1 + (g_1 + \sqrt{D_L}) \gamma} - R_d, \quad (4a)$$

$$g_c = \frac{A_n}{c_a - c_i} = \frac{g_l + \sqrt{D_L}}{c_a \sqrt{D_L}} \left[f_0 \frac{c_a g_l - (g_l + \sqrt{D_L}) \Gamma^*}{c_a g_l + (g_l + \sqrt{D_L}) \gamma} - R_d \right], \quad (4b)$$

$$E = g_w \frac{D_L}{P_{atm}} = 1.6 g_c \frac{D_L}{P_{atm}} = 1.6 \frac{g_l \sqrt{D_L} + D_L}{c_a P_{atm}} \left[f_0 \frac{c_a g_l - (g_l + \sqrt{D_L}) \Gamma^*}{c_a g_l + (g_l + \sqrt{D_L}) \gamma} - R_d \right], \quad (4c)$$

$$\text{WUE} = \frac{A_n}{E} = \frac{c_a P_{atm}}{1.6(g_l \sqrt{D_L} + D_L)}, \quad (4d)$$

where P_{atm} is the atmospheric pressure (kPa). For the Farquhar, von Caemmerer and Berry (1980) photosynthesis model, $f_0 = V_{c,max}$ and $\gamma = K_c \times (1 + o_i/K_o)$ under carboxylation-limited conditions, where $V_{c,max}$ is the maximum carboxylation rate ($\text{mol m}^{-2} \text{s}^{-1}$), K_c (mol mol^{-1}) and K_o (mol mol^{-1}) are Michaelis–Menten constants for carboxylation and oxygenation, and o_i is the leaf intercellular O_2 partial pressure (mol mol^{-1}), while under electron transport-limited conditions, $f_0 = J/4$ and $\gamma = 2\Gamma^*$, where J is the electron transport rate ($\text{mol m}^{-2} \text{s}^{-1}$).

In addition to its role in empirical stomatal models (Equation 1), g_l plays a role in constraining the form of stomatal optimality models. Optimality-based approaches, such as the classic optimization theory of Cowan and Farquhar (1977) and its approximation by Medlyn et al. (2011), have recently been called for to improve predictions of plant functioning and gas exchange, especially under novel environmental conditions (Franklin et al. 2020; Harrison et al. 2021). Indeed, stomatal optimality models are gradually replacing empirical relationships in large-scale ecosystem models (De Kauwe et al. 2015; Eller et al. 2020; Sabot et al. 2020; Wang and Frankenberg 2022). Stomata optimality models predict the stomatal conductance that maximizes some objective representing fitness (often of the form $A_n - \Theta$, where Θ is some assumed hydraulic cost; e.g., loss of soil–plant hydraulic conductance). When stomata behave optimally, the *marginal carbon cost of water* (i.e., $\partial\Theta/\partial E$ when maximizing $A_n - \Theta$)—a property of the optimization problem itself—equals the *marginal carbon profit of water* ($\partial A_n/\partial E$)—a property of gas exchange and photosynthesis that is independent of the optimization problem (Buckley, Sack, and Farquhar 2017; Potkay and Feng 2023b). The *marginal profit* is the ratio of the change in net carbon assimilation (∂A_n) to the change in transpiration (∂E) that would result if stomatal conductance changed while all else is held constant. It may be estimated from gas exchange measurements using various mathematical expressions (Buckley, Sack, and Farquhar 2017; Liang et al. 2023; Potkay and Feng 2023a, 2023b). For example, under the simplifying assumptions of negligible mesophyll and boundary layer resistances, Buckley, Sack and Farquhar (2017) derived a simple expression relating the *marginal profit* to leaf gas exchange rates and WUE,

$$\frac{\partial A_n}{\partial E} = \frac{k}{k + g_c} \frac{A_n}{E} = \frac{k}{k + g_c} \text{WUE}, \quad (5)$$

where $k = \partial A_n/\partial c_i$ is the slope of the biochemical A_n versus c_i curve at constant temperature. Like WUE, smaller $\partial A_n/\partial E$ is linked to larger g_c , A_n , and E . The generic biochemical carbon fixation model used above yields $k = f_0 \times (\Gamma^* + \gamma)/(c_i + \gamma)^2$.

To realize the potential for stomatal optimality models, it is essential to understand how the *marginal profit* responds to novel conditions under global environmental change. Few studies have examined how the *marginal profit* varies (Table 1), currently leaving the exact form of the objective of stomata optimality models up for debate (Wang et al. 2020; Sabot et al. 2022). Various theories assume different objectives, leading to different solutions for the *marginal cost* and thus also for the optimal stomatal conductance. For example, in Cowan and Farquhar's (1977) theory, the *marginal cost* is strictly constant. Conversely, recent optimality models often predict that the *marginal cost* rises as D_L decreases, as CO_2 concentrations increase, as soil water or hydraulic stress increase, and as photosynthetic photon flux density (PPFD) increases (Wang et al. 2020). Most recent models predict that the *marginal cost* changes immediately as environmental conditions change (Wang et al. 2020), while others predict delayed changes resulting from acclimation of structural growth and non-structural carbohydrate storage (Buckley and Schymanski 2014; Potkay and Feng 2023a, 2023b) or from dynamic changes in soil water availability (Mäkelä 1996; Manzoni et al. 2013; Mrad et al. 2019). It is essential to understand how the *marginal profit* varies empirically, especially under novel conditions associated with global environmental change, to inform the choice of objective of stomatal optimality models and thus to improve predictions of plant gas exchange and performance. The USO model's g_l parameter is a promising metric for studying how the *marginal profit* varies because, according to Medlyn et al. (2011), the two terms are related as

$$g_l = \sqrt{\frac{3\Gamma^* P_{atm}}{1.6 \frac{\partial A_n}{\partial E}}}. \quad (6)$$

To infer g_l , the standard practice has been to apply a simple linear regression between $g_c - A_n/c_a$ versus $A_n/(c_a D_L^{0.5})$ or equivalent expressions (Lamour et al. 2022; Davidson et al. 2023a, 2023b) to estimate g_l as the slope of Equation 1. Such regression yields a single, constant value for g_l . However, by assuming a constant g_l within a pool of observations, this regression-based approach confounds the difference between $\partial A_n/\partial g_c$ (an instantaneous derivative that is a part of the true slope) and A_n/g_c (a constant ratio), which are not equivalent (Buckley, Sack, and Farquhar 2002, 2017), and confounds the difference between their respective influences on the estimated slope (Liang et al. 2023). Resolving $\partial A_n/\partial g_c$ requires assuming changes in g_c are the only source of variation in A_n , while real data includes other sources of variations in A_n like changes in environmental conditions and photosynthetic capacities (Liang et al. 2023). This confusion between the interpretation of $\partial A_n/\partial g_c$ versus A_n/g_c has been termed the “ $A_n:g_c$ trap” and shown to result in up to 60% error in the estimate of g_l (Liang et al. 2023).

Instead of linear regression, many studies use non-linear solvers to fit the constant g_l that minimizes the errors between observed and predicted stomatal conductance (Héroult et al. 2013; Duursma 2015, Lin et al. 2015; Medlyn et al. 2017; Gimeno et al. 2016, 2019; Stefanski et al. 2023). Some ecosystem-scale studies bin data by soil moisture classes and fit a constant g_l to each bin (Lin et al. 2018; Sloan and Feng 2023), and others fit alternative empirical formulations for g_w to data binned by both leaf-to-air or atmospheric VPD

TABLE 1 | Examples of leaf-scale regression-based and inversion-based studies that test for effects of environmental or physiological drivers on g_1 or the *marginal carbon profit of water* ($\partial A_n/\partial E$).

Environmental or physiological driver	Inversion-based studies finding a significant effect of the driver on g_1 or $\partial A_n/\partial E$	Regression-based studies finding a weak or absent effect of the driver on g_1
Leaf-to-air vapor pressure deficit	Hall and Schulze (1980; $\partial A_n/\partial E$) Fites and Teskey (1988; $\partial A_n/\partial E$) Grieu, Guehl and Aussennac (1988; $\partial A_n/\partial E$) Thomas, Eamus and Bell (1999; $\partial A_n/\partial E$) Bloomfield et al. (2019; g_1) ^a Dong et al. (2020; g_1) ^a	—
Photosynthetic photon flux density (PPFD)	Thomas, Eamus and Bell (1999; $\partial A_n/\partial E$)	—
Atmospheric CO ₂ concentration	Katul et al. (2010; $\partial A_n/\partial E$) Manzoni et al. (2011; $\partial A_n/\partial E$)	Duursma et al. (2013) Gimeno et al. (2016) Gardner et al. (2023)
Soil moisture	Hall and Schulze (1980; $\partial A_n/\partial E$)	—
Midday leaf water potential	Manzoni et al. (2011; $\partial A_n/\partial E$)	—
Predawn leaf water potential	Grieu, Guehl and Aussennac (1988; $\partial A_n/\partial E$) Thomas, Eamus and Bell (1999; $\partial A_n/\partial E$) Zhou et al. (2013, 2014, 2016; g_1) Drake et al. (2017; g_1)	Gimeno et al. (2016) Davidson et al. (2023a)
Temperature ^{b,c}	Wang et al. (2017; g_1) ^a Bloomfield et al. (2019; g_1) ^a Dong et al. (2020; g_1)	Duursma et al. (2013) Gimeno et al. (2016) Stefanski et al. (2023)

^aWang et al. (2017), Bloomfield et al. (2019), and Dong et al. (2020) report the effects of VPD and temperature on g_1 from multiple linear regression of point estimates of the ratio of the leaf internal to atmospheric CO₂ partial pressure (c_v/c_a ; Equation 2) derived from bulk leaf carbon isotopes.

^bEven though $\partial A_n/\partial E$ remains constant with leaf temperature (Hall and Schulze 1980; Thomas, Eamus, and Bell 1999), g_1 is expected to vary with leaf temperature according to Medlyn et al. (2011), since g_1 is a function of the temperature-dependent CO₂ compensation point (I^* ; Equation 6) (Bernacchi et al. 2001). The alternative stomatal optimization hypothesis of Prentice et al. (2014) proposes that g_1 varies with leaf temperature, being proportional to the square-root of the effective Michaelis-Menten coefficient for carboxylation-limited photosynthetic net carbon assimilation [i.e., $K_c \cdot (1 + o_0/K_o)$] and to the square-root of the viscosity of water, both of which are temperature-dependent.

^cSome regression-based studies have indeed found an effect of temperature on g_1 at extreme temperatures (Marchin et al. 2016, 2023; Urban et al. 2017; Aparecido et al. 2020).

and soil moisture (Novick et al. 2016; Li et al. 2019). Like linear regression, this approach assumes constant g_1 within each bin or treatment and thus cannot detect variations in g_1 within a bin or treatment. Hence, these studies perform a form of regression that is similarly susceptible to the “ A_n ; g_c trap” as simple linear regression.

Here, we explore the accuracy of an alternate approach to estimating g_1 through direct inversion of the stomatal conductance model, specifically under changing environmental conditions that affect A_n (and thus $\partial A_n/\partial g_c$). The inversion-based approach estimates g_1 directly by rearranging Equation 1 and disregarding g_0 ,

$$g_1 = \sqrt{D_L} \left(\frac{g_c c_a}{A_n} - 1 \right), \quad (7)$$

producing point estimates of g_1 for each observation (simultaneous A_n , g_c , c_a , and D_L) that may be statistically modeled against physiological and environmental conditions to explain variations in g_1 and thus also $\partial A_n/\partial E$. Inversion-based studies often report that g_1 and the *marginal profit* ($\partial A_n/\partial E$)

vary over short periods (hours to months) as conditions change (Table 1). These results often conflict with small or negligible differences in g_1 between experimental treatments from regression-based leaf-level studies (Table 1), in which environmental and physiological effects on g_1 are typically analyzed by (1) binning gas exchange data by experimental treatment, (2) determining a single g_1 by (either simple linear or non-linear) regression within each bin, and (3) testing for significant differences between the g_1 of each treatment (often through mixed-effects models). These conflicting reports on whether and how g_1 varies need to be resolved to advance both empirical and optimality-based stomatal models and thus to improve predictions of leaf-level gas exchange and plant functioning.

To evaluate their performance for estimating stomata slope parameters, we ask three questions related to the precision and accuracy of the regression- and inversion-based approaches under varying g_1 . Specifically, (1) can a hypothetical “observer” tell that g_1 actually varies based on the quality of the fit of a regression (e.g., R^2 between $g_c - A_n/c_a$ and $A_n/(c_a D_L^{0.5})$)? (2) When g_1 actually varies, how well can A_n be predicted from a constant g_1 estimated by

regression? (3) Does the inversion method (Equation 7 & statistical modeling of g_1) improve predictions of A_n ? We present a hypothetical thought experiment to answer our questions. We hypothesize that regressed g_1 will perform worse when the actual g_1 is more sensitive to varying conditions. Based on our thought experiment, we recommend that point estimates of g_1 be determined by inversion in future studies, from which the environmental sensitivity of g_1 can be directly analyzed through statistical approaches.

2 | Materials and Methods

2.1 | Model Setup

We simulate the gas exchange for 20 species from Zhou et al. (2013) Table S1 using a gas exchange model from our previous work (Potkay and Feng 2023a, 2023b) modified to use the USO (Equations 1 and 4) and assume carboxylation-limited photosynthesis (Farquhar, von Caemmerer, and Berry 1980). To answer Question 1 whether an “observer” could tell that g_1 varies from the regression approach, g_1 must vary with environmental conditions (soil moisture, temperature, light, CO_2). However, only one source of variation is necessary to answer Question 1. For simplicity, we consider predawn water potential (ψ_{pd}) as the single source of g_1 variation using the parameters provided by Zhou et al. (2013) Table S1 because the mathematical relationships between point-estimate-derived g_1 (or $\partial A_n / \partial E$) and hydraulic variables are well established (Manzoni et al. 2011; Zhou, Medlyn, and Prentice 2013, 2014, 2016; Drake et al. 2017; Equation 8 below). Conversely, far less is known about the relationships between g_1 and other environmental variables. Accordingly, we assume constant D_L (1 kPa), c_a (410 $\mu\text{mol mol}^{-1}$), and leaf temperature and thus do not consider the temperature dependencies of photosynthetic parameters (Bernacchi et al. 2001). We also assume negligible boundary layer and mesophyll resistances and that $g_0 = 0 \text{ mol m}^{-2} \text{ s}^{-1}$. We set $I^* = 42.75 \mu\text{mol mol}^{-1}$, $P_{atm} = 101.325 \text{ kPa}$, the leaf internal O_2 partial pressure (o_i) to 207 mmol mol^{-1} , the Michaelis-Menten coefficients for carbon fixation and oxygen inhibition (K_c & K_o) to 404.9 $\mu\text{mol mol}^{-1}$ and 278.4 mmol mol^{-1} , respectively, and the leaf dark respiration (R_d ; $\text{mol m}^{-2} \text{ s}^{-1}$) to 0.01· $V_{c,max,0}$ (De Pury and Farquhar 1997).

Like Zhou, Medlyn, and Prentice (2013, 2014, 2016) and Drake et al. (2017), we model g_1 as an exponential function of ψ_{pd} ,

$$g_1 = a \exp(b\psi_{pd}), \quad (8)$$

where a is the value of g_1 when $\psi_{pd} = 0$ ($\text{kPa}^{0.5}$), and b is the sensitivity of g_1 to ψ_{pd} (MPa^{-1}). The maximum carboxylation rate ($V_{c,max}$; $\text{mol m}^{-2} \text{ s}^{-1}$) is modeled as a sigmoidal function of ψ_{pd} , following Tuzet et al. (2003),

$$V_{c,max} = V_{c,max,0} \frac{1 + \exp(S_f \psi_f)}{1 + \exp[S_f(\psi_f - \psi_{pd})]}, \quad (9)$$

where $V_{c,max,0}$ is the value of $V_{c,max}$ when $\psi_{pd} = 0$ ($\text{mol m}^{-2} \text{ s}^{-1}$), and S_f (MPa^{-1}) and ψ_f (MPa) are shape parameters controlling the decline in $V_{c,max}$ as ψ_{pd} becomes more negative. For each species, we simulate gas exchange (e.g., g_c , A_n) starting at

$\psi_{pd} = 0 \text{ MPa}$ using Equations 8 and 9 for g_1 and $V_{c,max}$ and progressively decreasing ψ_{pd} by 0.002 MPa increments until $g_c = 0 \text{ mol m}^{-2} \text{ s}^{-1}$, meaning that species experienced different ψ_{pd} ranges. Although entirely simulated, we consider these values of g_1 (Equation 8) and A_n (from our gas exchange model with Equations 8 and 9) (Figure 1) as “observations.” Subsequent predictions based on regression and inversion of these values as merely “estimates”, which we denote by \hat{g}_1 and \hat{A}_n for regression and \tilde{g}_1 and \tilde{A}_n for inversion.

2.2 | Estimated R^2 , Slope Parameters, Gas Exchange, and Error

Once A_n and g_c were calculated across a suite of ψ_{pd} values, we plotted $g_c - A_n/c_a$ against $A_n/(c_a D_L^{0.5})$ (Figure 1). From these curves, we calculated three regression-based estimates of g_1 (i.e., \hat{g}_1) and their associated coefficient of determination (R^2). We estimated \hat{g}_1 as the slope of the $g_c - A_n/c_a$ versus $A_n/(c_a D_L^{0.5})$ curves, forcing the intercept to zero ($g_0 = 0 \text{ mol m}^{-2} \text{ s}^{-1}$). The first set of R^2 and regression-based \hat{g}_1 were estimated from all simulated datapoints. Unless performed in a highly controlled experiment to encompass a broad range of predawn water potentials, the hypothetical observer is unlikely to observe the entire range of ψ_{pd} , and hence two other sets of R^2 and regression-based \hat{g}_1 were estimated from a subset of six randomly chosen datapoints, repeating the process 1000 times. Six was chosen as the subset size, since some studies estimate g_1 by regression with an average of six datapoints (Stefanski et al. 2023). Six datapoints were randomly sampled by two approaches. First, datapoints were sampled uniformly, and datapoints had equal probabilities of being chosen. Second, datapoints were sampled based on the theoretical probability distribution of ψ_{pd} for stochastic rainfall events with a realistic mean frequency (λ ; s^{-1}) of 0.2 day $^{-1}$ and mean rainfall depth (α ; m) of 1 cm (Rodriguez-Iturbe et al. 1990) called the ecohydrological distribution (Notes S1 in Supporting Information). This ecohydrological distribution represents a more realistic probability distribution for ψ_{pd} than the uniform distribution. For simplicity, when calculating the ecohydrological distributions, all species were assumed to share the same soil properties, leaf area indices, and rooting depths using trait values that are representative of many species and soil parameters that are representative of loamy soil (Rodriguez-Iturbe and Porporato 2004).

Additionally, we estimated g_1 by inversion (i.e., \tilde{g}_1 ; Equation 7). These point estimates of g_1 are identical to the “true” values from Equation 8. Hence, we consider only the case for observing a limited subset of six datapoints, since inversion would lead to zero error if an entire $g_c - A_n/c_a$ versus $A_n/(c_a D_L^{0.5})$ curve (Figure 1) were observed. For inversion, error arises from how variations in \tilde{g}_1 are interpolated or extrapolated for unobserved conditions. We randomly sampled six estimates of inversion-based \tilde{g}_1 according to either the uniform or ecohydrological distribution. These estimates were statistically modeled as an exponential (Equation 8) or a second-order polynomial function of ψ_{pd} to recapture the original dependence of g_1 on ψ_{pd} . This procedure was repeated 1000 times. When modeling \tilde{g}_1 as an exponential function, errors should be small, since the form for the statistical model matches the functional form of the “true” g_1 (Equation 8). We considered the second-order polynomial function, because it has a different form than that of the “true”

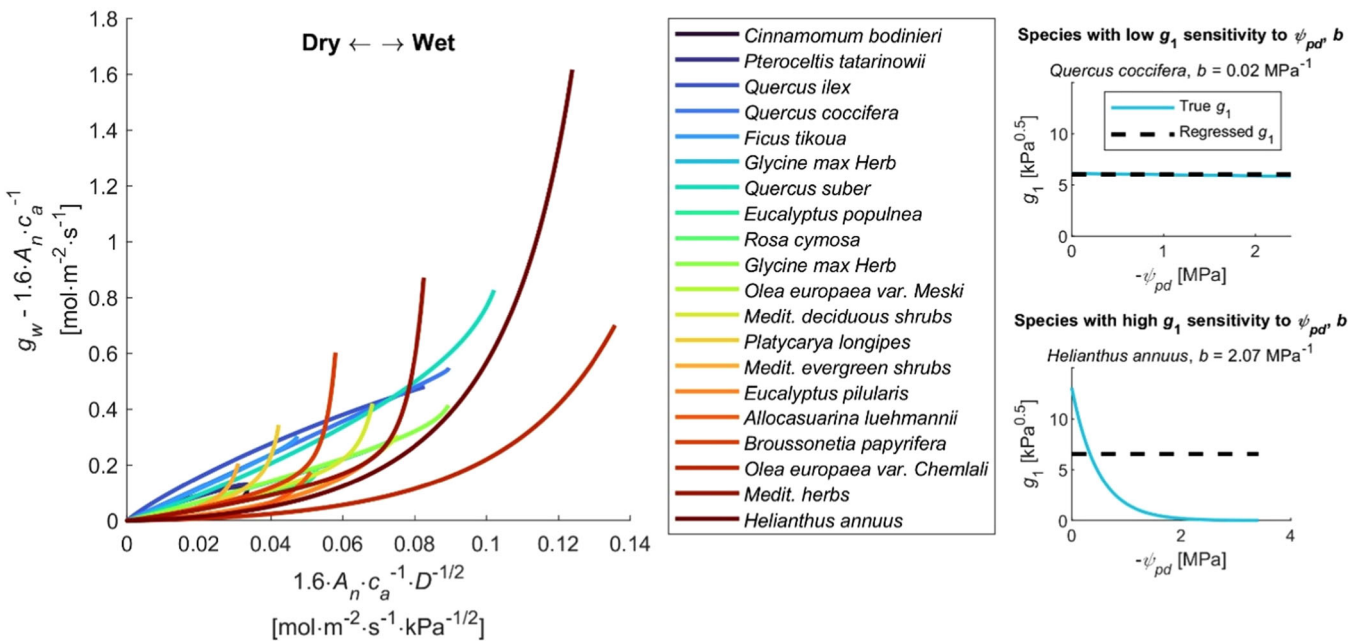


FIGURE 1 | On the left, values of $1.6 \cdot A_n / (c_a D_L^{0.5})$ on the x-axis against $g_w - 1.6 \cdot A_n / c_a$ on the y-axis simulated by varying predawn water potential (ψ_{pd}) for 20 species using parameters reported by Zhou et al. (2013). The upper right and lower left portions of the plot reflect wetter conditions (less negative ψ_{pd}) and drier conditions (more negative ψ_{pd}), respectively. Species are ordered in the legend according to the sensitivity of g_1 to ψ_{pd} (b in Equation 8) with the least and most sensitive species listed at the top and bottom of the legend, respectively. The slope of each line is the corresponding specie's value of g_1 . On the right, comparisons between the true ψ_{pd} -dependent g_1 and the constant g_1 estimated by regression for species with small and large b in the top and bottom, respectively. The regressed g_1 compares well to the true g_1 when b is small. However, regression underestimates and overestimates g_1 under wet and dry conditions, respectively, when b is large. [Color figure can be viewed at wileyonlinelibrary.com]

g_1 . Since it is prone to errors upon extrapolation, if statistical modeling of inversion-based \hat{g}_1 as a polynomial of ψ_{pd} were to perform better than regression, it would show that even using wrong functional forms outperform regression. We note that regression is applied during the inversion approach *a posteriori* only to explain the variations in \tilde{g}_1 with respect to ψ_{pd} . This application is fundamentally different from the regression-based approach that infers \hat{g}_1 by regression.

To assess the abilities of the regression- versus inversion-based g_1 estimates to predict A_n (Questions 2 and 3), we used our gas exchange model to calculate \hat{A}_n and \tilde{A}_n across the full range of ψ_{pd} using the constant regression-based \hat{g}_1 and the \tilde{g}_1 predicted by the statistical models fitted from inversion-based point estimates. We quantify the total difference between the “true” A_n and “estimated” \hat{A}_n and \tilde{A}_n across a range of expected ψ_{pd} through the relative root mean square error (RRMSE),

$$\text{RRMSE} = \sqrt{\frac{\int_{-\infty}^0 (A_n(\psi_{pd}) - \tilde{A}_n(\psi_{pd}))^2 p(\psi_{pd}) d\psi_{pd}}{\int_{-\infty}^0 A_n(\psi_{pd})^2 p(\psi_{pd}) d\psi_{pd}}}, \quad (10)$$

where $p(\psi_{pd})$ is the probability distribution of predawn water potentials, being either uniform or ecohydrological, and \tilde{A}_n is the “estimated” net carbon assimilation rate (either \hat{A}_n or \tilde{A}_n). Even though regression-based \hat{g}_1 are constant and thus independent of ψ_{pd} , \hat{A}_n still depends on ψ_{pd} through the sensitivity of $V_{c,max}$ to ψ_{pd} (Equation 9). For \hat{g}_1 estimated by regressing an entire curve in Figure 1, we report two values of RRMSE, one for each of the

distributions for ψ_{pd} . For \hat{g}_1 and \tilde{g}_1 estimated from small data subsets, we made 1000 predictions of how \hat{A}_n and \tilde{A}_n vary with ψ_{pd} , since the random subsampling was repeated 1000 times. To avoid 1000 RRMSE values, we calculated RRMSE based on the mean responses of \hat{A}_n and \tilde{A}_n to ψ_{pd} .

2.3 | Scenario Exploration

To answer Question 1 whether a hypothetical “observer” could tell that g_1 varied from the quality of fit of linear regression, we analyze the R^2 between $g_c - A_n / c_a$ and $A_n / (c_a D_L^{0.5})$ using their “true” values. R^2 quantifies the linearity of the relationship (i.e., variance explained by the linear model), thus high R^2 values would suggest that g_1 is constant, and low R^2 values would suggest that g_1 varies with ψ_{pd} . While R^2 is not the best metric of linearity, few leaf-level studies report performing other tests of linearity like checking residuals for normality and heteroscedasticity (Lamour et al. 2022), and R^2 is the most common metric of fit quality in leaf-level studies. For simplicity, our analysis considers only the variation of ψ_{pd} , since the necessary parameters were available (a , b , $V_{c,max,0}$, S_f , ψ_f , Table S1), but our conclusions for Question 1 extend to cases in which other environmental conditions vary since Question 1 asks whether the regression approach can detect variations in g_1 regardless of the exact source of variation. To answer Question 2 whether a constant \hat{g}_1 estimated by regression can accurately predict A_n when the “true” g_1 varies and Question 3 whether the inversion method improves predictions of A_n , we compared the “true” A_n to the \hat{A}_n estimates predicted by the regressed \hat{g}_1 and to \tilde{A}_n from the statistically modeled inversion-based \tilde{g}_1 and analyzed their corresponding RRMSEs.

3 | Results and Discussion

3.1 | Regression Obscures Effects of Environmental Variation on Stomatal Response

Figure 1 shows the values of $g_c - A_n/c_a$ plotted against $A_n/(c_a D_L^{0.5})$ simulated by varying ψ_{pd} for 20 species (Zhou et al. 2013; Table S1), from which \hat{g}_1 is traditionally estimated by regression as the slope. Wetter conditions (less negative ψ_{pd}) and drier conditions (more negative ψ_{pd}) are represented by the upper right and lower left portions of Figure 1. For species with g_1 more sensitive to ψ_{pd} (larger absolute value of $b, |b|$), the curves are more nonlinear (Figure 1). The nonlinearity is further demonstrated by a general decline in R^2 as $|b|$ increases (Figure 2 & S1). When considering the full range of ψ_{pd} , R^2 is near 1 for species with $0 \leq b \leq -0.5 \text{ MPa}^{-1}$ and declines to ~ 0.7 for the largest considered value of b ($\sim 2 \text{ MPa}^{-1}$). When choosing limited subsets of six datapoints from the uniform and ecohydrological distributions, median R^2 similarly declines as $|b|$ increases and is always higher than the R^2 estimated for the complete dataset (Figure 2), consistent with reports that R^2 is biased upward for small sample sizes (Cramer 1987). The minimum value of R^2 of 0.67 is not small enough to guarantee that a hypothetical “observer” would correctly discount the $g_c - A_n/c_a$ versus $A_n/(c_a D_L^{0.5})$ relationship as linear, because an R^2 of 0.7 or higher suggests a high level of correlation for ecological studies. The “observer” is likely to wrongly assume that the R^2 is not higher because of randomness and noise in the data rather than correctly ascribing it to variation in g_1 . Unless performing a highly controlled experiment to encompass a

broad range of ψ_{pd} , the “observer” is likely to observe an incomplete sample, and they would observe an R^2 larger than 0.7 (blue and red violin plots in Figure 2), leading to overconfidence in their model’s performance and in the linearity of the $g_c - A_n/c_a$ versus $A_n/(c_a D_L^{0.5})$ relationship. While R^2 indeed declines as $|b|$ increases, the answer to Question 1 is that the “observer” would likely conclude that fitting each of the curves in Figure 1 with a constant slope is justified and proceed with regression, ignoring potential variation in g_1 , regardless of how sensitive g_1 is to ψ_{pd} (b).

3.2 | Potential for Large Errors in Gas Exchange Predictions Using Regressed Slope Parameters

Predictions of \hat{A}_n from the regressed \hat{g}_1 compared well to the “true” A_n for species with small b ; however, \hat{A}_n diverged from A_n for species with large $|b|$ (Figure 3; Figures S2 and S3). The RRMSE for \hat{A}_n predicted for \hat{g}_1 regressed from the entire $g_c - A_n/c_a$ versus $A_n/(c_a D_L^{0.5})$ curve (Figure 3) was on average slightly higher than the RRMSE for \hat{A}_n predicted for \hat{g}_1 regressed from a limited subset of six datapoints (Figure S2), since RRMSE is biased towards better performance for smaller sample sizes due to their biases in standard deviation (Holtzman 1950) like R^2 . The ecohydrological distribution was generally prone to more error than the uniform distribution, regardless of whether \hat{g}_1 was regressed from the entire curve (Figure 3) or a limited data subset (Figure S2). For *Helianthus annuus*, the species with the largest b of 2.07 (Table S1), RRMSE for \hat{A}_n predicted for \hat{g}_1 regressed from the entire curve was 27% and 65% for the

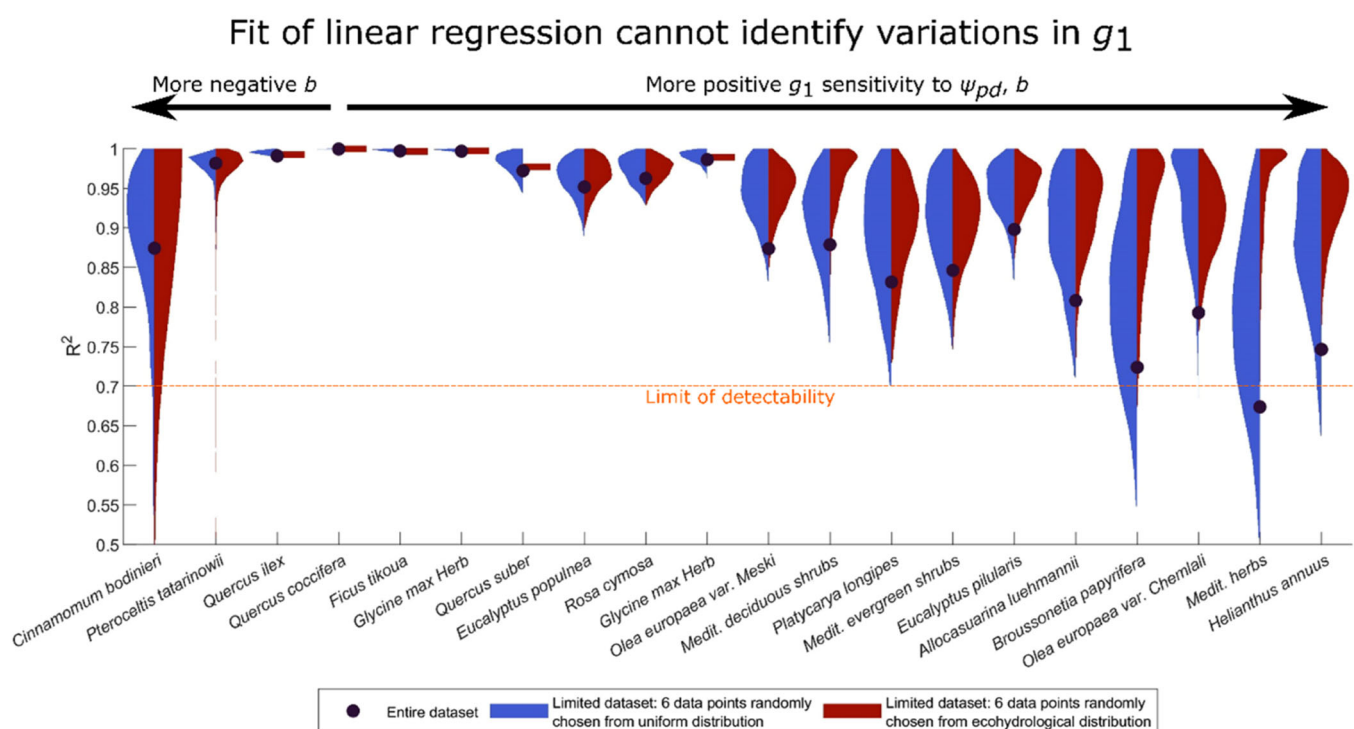


FIGURE 2 | R^2 between the $g_w - 1.6 \times A_n/c_a$ and $1.6 \times A_n/(c_a D_L^{0.5})$ values showed in Figure 1. Species are ordered from left to right according to the sensitivity of g_1 to ψ_{pd} (b in Equation 8). Black circles show the R^2 determined for the entirety of each line in Figure 1. Blue and red violin plots show the distribution of R^2 determined from randomly choosing six datapoints, repeated 1000 times, chosen by a uniform and ecohydrological distribution of ψ_{pd} , respectively. Violin plots are replaced with thick lines when R^2 is singularly distributed. [Color figure can be viewed at wileyonlinelibrary.com]

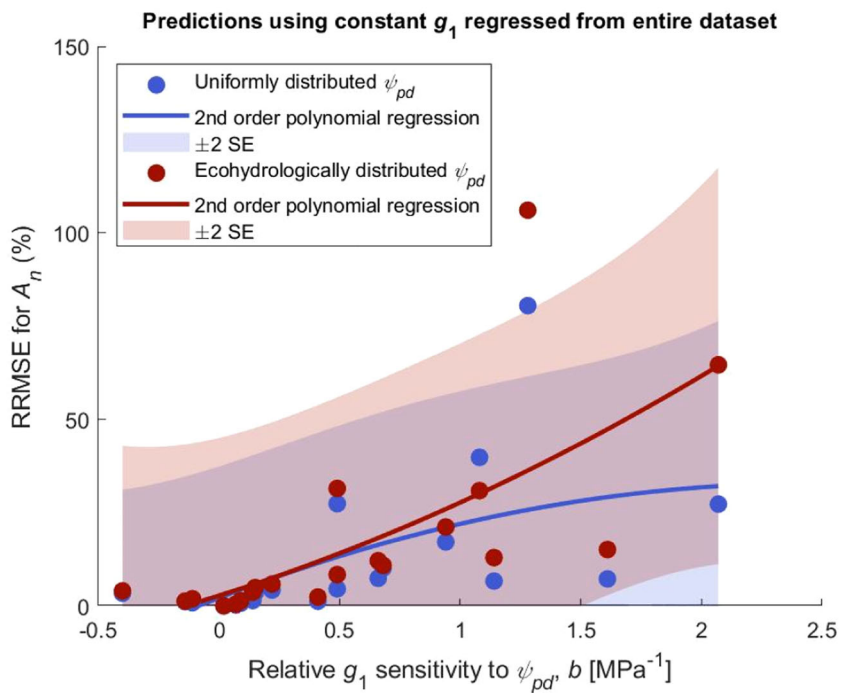


FIGURE 3 | Relative root mean square error (RRMSE; circles) for A_n against the relative sensitivity of g_1 to predawn water potential (b in Equation 8). Comparison of “true” A_n to \hat{A}_n predicted from \hat{g}_1 estimated by regressing the complete $g_c - A_n/c_a$ versus $A_n/(c_a D_L^{0.5})$ curve for each species. Lines are 2nd order polynomial fits to RRMSE in terms of b , and shaded areas shows ± 2 standard errors (SE) of the fit. [Color figure can be viewed at wileyonlinelibrary.com]

uniform and ecohydrological distributions, respectively (Figure 3). For \hat{A}_n predicted for \hat{g}_1 regressed from a limited subset, RRMSE was 24% and 41% for the uniform and ecohydrological distributions, respectively (Figure S2). The largest errors occurred for *Olea europaea* var. *Chemlali*, a species with a moderate b of 1.28 but with the lowest sensitivity of $V_{c,max}$ to ψ_{pd} (S_f in Equation 9) of the considered species (Table S1). For \hat{g}_1 regressed from the entire curve, the RRMSE for *Olea europaea* var. *Chemlali* was 80% and 106% for the uniform and ecohydrological distributions, respectively (Figure 3), while for \hat{g}_1 regressed from a limited data subset, the RRMSE was 63% and 77% for the uniform and ecohydrological distributions, respectively (Figure S2), suggesting that the problems of regression are exacerbated for species with moderate to large b and small S_f . Conversely, greater sensitivity of $V_{c,max}$ to ψ_{pd} (large S_f) effectively conceals some of the error of assuming a constant g_1 for species with larger b , because as ψ_{pd} become more negative and as stomata close for species with large S_f , declines in $V_{c,max}$ become responsible for more decline in A_n (independently of g_1 variations), and less change in g_1 is required to capture stomatal closure (i.e., constant \hat{g}_1 becomes more acceptable). The answer to Question 2 is that estimating \hat{g}_1 by regression can cause large errors for predicting \hat{A}_n as high as 106%.

3.3 | Inversion Improves Gas Exchange Predictions

Inverting a limited number of point estimates of g_1 (i.e., \tilde{g}_1) and statistically modeling them as a function of ψ_{pd} resulted in less error than estimating \hat{g}_1 by regression when predicting A_n

(Figure 3; Figures S2, S4, S5). When statistically modeling the \tilde{g}_1 point estimates as an exponential function of ψ_{pd} (Equation 8), errors for \hat{A}_n were virtually absent, never exceeding 1% (Figures S4 and S6). This result was expected because both the relationship between the “true” g_1 and ψ_{pd} and the relationship between the statistically modeled \tilde{g}_1 point estimates and ψ_{pd} share the same exponential form. More errors would have been introduced if the statistical model differed in functional form from the “true” relationship. Hence, we also fitted second-order polynomial functions to the subsets of \tilde{g}_1 point estimates. These second-order polynomial functions represent an extreme case because they can resemble the “true” exponential function over small intervals, but they can also predict unrealistic responses for \tilde{g}_1 when extrapolating to unobserved conditions (e.g., nonmonotonic \tilde{g}_1 - ψ_{pd} fits). Nonetheless, despite its limitations, modeling the \tilde{g}_1 point estimates as a second-order polynomial function resulted in less error than regression-based predictions (Figures S5 and S7), because the second-order polynomial statistical models can capture some of the variations of \tilde{g}_1 with respect to ψ_{pd} , whereas the regressed \hat{g}_1 is constant and cannot capture variations. These results emphasize the improvements in gas exchange predictions that can be made by capturing even just some of the variations in g_1 .

When uniformly sampled, RRMSE was largest for *Olea europaea* var. *Chemlali* (Figure S5), like for with regressed \hat{g}_1 (Figures 3 and S2), at 30%, less than half of any of the RRMSE values for *Olea europaea* var. *Chemlali* with regressed \hat{g}_1 . For the ecohydrologically distributed data, RRMSE was largest for *Cinnamomum bodinieri*, the only considered species with negative b (Table S1), at 22% (Figure S5). Because of

Cinnamomum bodinieri's negative b , its ecohydrological probability distribution is heavily skewed towards ψ_{pd} near zero, guaranteeing error for unobserved dry conditions. Besides these exceptions, RRMSE was always less than 10% (Figure S5). Overall, the answer to Question 3 is that the inversion method (Equation 7 and statistical modeling of point estimates) does indeed improve predictions of A_n compared to the traditional regression approach that assumes constant g_1 , even when statistically modeling \tilde{g}_1 point estimates with dubious functional forms like second-order polynomials, which can predict unrealistic g_1 responses upon extrapolation.

3.4 | A Proposed Roadmap for Identifying Environmental Controls on Slope Parameters

While the traditional approach of estimating stomatal slope parameters (g_1) by linear regression may appear justified (i.e., high R^2 ; Figure 2), regression conceals variations in g_1 , making it difficult to interpret how g_1 varies with environmental and physiological conditions. This result may explain why regression-based studies frequently report small differences between single g_1 values regressed from different treatments, while inversion-based studies often find clear effects (Table 1). Not considering the variations in g_1 can lead to large errors for A_n (as high as 106% for our considered species; Figure 3), especially for species with highly variable g_1 and low variation in photosynthetic capacities.

We recommend that future studies estimate g_1 by inversion (Equation 2 or 7). Statistical models for g_1 can be constructed through structural equation (Zhai et al. 2024) and mixed-effects (Lin et al. 2015) modeling. Based on previously observed and theorized responses of g_1 and the *marginal profit* to environmental and physiological conditions (Katul et al. 2010; Manzoni et al. 2011; Zhou, Medlyn, and Prentice 2013, 2014, 2016; Nakad et al. 2023; Table 1), explanatory variables should include c_a , leaf temperature, and a hydraulic variable (e.g., soil water content, soil water potential, midday or predawn leaf water potential). We propose that the fixed effects of linear mixed-effects models for the logarithmically transformed g_1 be structured as

$$\log(g_1) \sim 1 + \log(c_a) + \log(T_L^K) + \psi_L, \quad (11)$$

with additional random effects from treatment and other appropriate groupings and additional fixed effects as needed. We justify the structure of Equation 11 in our SI (Equation S2.5, Notes S2). Alternatively, similar logarithmically transformed mixed-effects modeling may be performed on point estimates of the *marginal carbon profit of water* ($\partial A_n / \partial E$) calculated from leaf gas exchange measurements through equations provided by Buckley, Sack and Farquhar (2017; e.g., Equation 5) and Liang et al. (2023). The independent effects of environmental conditions on stomatal behavior can be concluded from effects (slopes) of the explanatory variables on either g_1 or $\partial A_n / \partial E$, thereby identifying what response stomatal optimality models should predict. Alternatively, other types of statistical modeling may be used

to explain variations in g_1 and $\partial A_n / \partial E$, like non-linear mixed-effects modeling (Lindstrom and Bates 1990) or machine learning methods (e.g., Shapley additive explanations; Lundberg and Lee 2017; artificial neural networks; Raghav, Kumar, and Liu 2024). Another option is to determine g_1 as the slope of the fixed effect of $A_n / (c_a D_L^{0.5})$ from linear mixed-effects modeling of $g_1 - A_n / c_a$ with treatment as a random effect; however, this approach is a form of regression and is thus prone to Liang et al.'s (2023) " A_n / c_a trap". Methods that allow for variation in g_1 with environmental and physiological conditions (within and among treatments) like ours avoid the problems of regression (within a single treatment) and of identifying the controls of g_1 from differences in treatments' mean g_1 .

3.5 | The Shared Variable Problem for Stomatal Responses to CO_2 and VPD

Caution must be taken when attempting to determine the effects of CO_2 concentrations or VPD on g_1 (or $\partial A_n / \partial E$) point estimates because of a 'shared variable problem'. Correlations between g_1 (or $\partial A_n / \partial E$) and either c_a or D_L may be spurious due to c_a and D_L appearing both in the calculation of g_1 (Equations 2 and 7) and as explanatory variables used to statistically model g_1 (Equation 11). The few attempts to find effects of either c_a or D_L on $\partial A_n / \partial E$ point estimates derived from gas exchange measurements and eddy covariance data have not considered this potential spuriousness (Hall and Schulze 1980; Fites and Teskey 1988; Grieu, Guehl, and Aussenac 1988; Thomas, Eamus, and Bell 1999; Katul et al. 2010; Yi et al. 2024). Statistical models for g_1 or $\partial A_n / \partial E$ with c_a or D_L as explanatory variables should be tested for spuriousness, such as comparing the observed Spearman's correlation coefficients between c_a or D_L and g_1 or $\partial A_n / \partial E$ to null correlations from randomization tests as described by Jackson and Somers (1991; see Wolfe et al. 2023 for example). A positive correlation between c_a and g_1 could indicate spuriousness because the effect of c_a on g_1 is positive in Equation 7 ($\partial g_1 / \partial c_a > 0$). Likewise, a negative correlation between D_L and g_1 could indicate spuriousness ($\partial g_1 / \partial D_L < 0$ because $g_1 = \sqrt{D_L} \left(\frac{g_c c_a}{A_n} - 1 \right) \approx \sqrt{D_L} \left(\frac{s_w c_a}{1.6 \times A_n} - 1 \right) = \sqrt{D_L} \left(\frac{E c_a}{1.6 \times D_L A_n} - 1 \right) = \left(\frac{E c_a}{1.6 \times \sqrt{D_L} A_n} - \sqrt{D_L} \right)$). Likewise, care should be taken when interpreting correlations between g_1 point estimates and leaf temperature. Such correlations may be spurious due to covariation between leaf and air temperatures (Michaletz et al. 2016), both of which determine the D_L (Grossiord et al. 2020) that is used to calculate g_1 .

We recommend an alternative approach to circumvent spurious correlations with CO_2 concentrations by estimating stomatal slope parameters (g_1) without c_a observations through ^{13}C isotope discrimination that provides estimates of the c_i / c_a ratio that can be plugged into Equation 2 (Medlyn et al. 2017). Similarly, ^{13}C discrimination measurements enable $\partial A_n / \partial E$ calculations without c_a when photosynthesis is light-limited (Liang et al. 2023). This approach typically uses ^{13}C discrimination of bulk leaf carbon (Medlyn et al. 2017; Wang et al. 2017; Bloomfield et al. 2019), providing a representative value of g_1 during the growth period (Cernusak et al. 2013) that may be larger (Bloomfield et al. 2019) or smaller (Medlyn et al. 2017) than

real-time g_1 point estimates from gas exchange measurements. Real-time g_1 point estimates may be calculated from ‘online’ ^{13}C discrimination values derived from the difference in the ^{13}C isotope composition of the air entering and leaving a leaf gas exchange chamber by the method of Evans et al. (1986). These g_1 point estimates could be statistically modeled in terms of c_a , avoiding the shared variable problem, to answer how CO_2 concentrations affect stomatal behavior. Hence, datasets of ‘online’ ^{13}C discrimination under experimentally varied c_a (Busch et al. 2020; Wang et al. 2024) will be critical to determining stomatal responses to c_a .

There are currently no means of detecting effects of VPD on g_1 and $\partial A_n / \partial E$ point estimates that entirely avoid the possibility of spurious correlations. The likelihood of spurious correlations would be reduced by rearranging Equation 2 and statistically modeling $\log\left(\frac{\frac{c_i}{c_a}}{1 - \frac{c_i}{c_a}}\right)$ instead of $\log(g_1)$ like Equation 11 with an additional fixed effect of $\log(D_L)$ (Equation S2.6, Notes S2; Wang et al. 2017; Bloomfield et al. 2019; Dong et al. 2020). However, spurious correlation would still be possible when analyzing gas exchange data in the absence of leaf ^{13}C isotope data, because the calculation of c_i depends on D_L (Long 2003). Like for CO_2 , datasets of ‘online’ ^{13}C discrimination under experimentally varied VPD (Cernusak et al. 2019; Holloway-Phillips et al. 2019; Wong et al. 2022; Diao et al. 2024) could determine how g_1 varies with D_L . Nonetheless, little empirical evidence suggests that g_1 and $\partial A_n / \partial E$ should vary with VPD since using constant g_1 and $\partial A_n / \partial E$ correctly predicts the response of stomatal conductance to VPD (Katul, Palmroth, and Oren 2009). Some eddy covariance and bulk leaf ^{13}C discrimination studies report correlations between g_1 and VPD. The eddy covariance studies modify the USO model, replacing the inverse-square-root of D_L (i.e., $\frac{1}{\sqrt{D_L}}$ in Equation 1) with an inverse-power law of D_L (i.e., $\frac{1}{D_L^m}$; Lin et al. 2018) with a fitted exponent (m) that would equal 0.5 if g_1 were independent of VPD. Several eddy covariance studies report exponents that are either larger or smaller than 0.5 (Lin et al. 2018, 2019; Liu et al. 2022), suggesting that g_1 may respectively decrease or increase with VPD. The bulk leaf ^{13}C discrimination studies estimate similar exponents, typically being greater than 0.5 (Bloomfield et al. 2019; Dong et al. 2020). However, these correlations cannot answer whether VPD directly or indirectly affects g_1 since they do not consider the effect of other covarying factors (e.g., Equation 11). For example, high VPD could cause more negative leaf water potentials that decrease g_1 . This nuance of direct versus indirect VPD-effects on g_1 is needed to constrain the form of stomatal models, particularly optimality-based models (Wang et al. 2020; Bassiouni and Vico 2021).

4 | Conclusion

We present the pitfalls of inferring g_1 from the traditional regression approach and recommend an alternate, more flexible inversion approach. The regression method cannot attribute variations in g_1 to variations in physiological and environmental conditions, potentially leading to large errors in net carbon assimilation that the inversion approach avoids. Their methodological differences may explain why regression- and inversion-based studies often report

different sensitivities of g_1 to environmental or physiological drivers (Table 1). By statistical modeling g_1 point estimates (e.g., Equation 11), the inversion approach can discern the sensitivity of g_1 to each of its drivers. Caution should be taken when determining the effects of CO_2 concentrations or VPD on g_1 point estimates due to potentially spurious correlations, although they may be circumvented by ^{13}C isotope measurements, especially those from Evans et al.’s (1986) ‘online’ method. An improved understanding of g_1 and how it varies will advance stomatal conductance models that are essential for predicting future carbon and water fluxes and plant performance under a changing climate, in part by constraining the form of stomatal optimality models.

Acknowledgements

A.P. was supported by the National Oceanic and Atmospheric Administration (NOAA) Climate & Global Change Postdoctoral Fellowship. X. F. was supported by a National Science Foundation Faculty Early Career Development (CAREER) award DEB-2045610. B.P.S. acknowledges support from the Center for Bioenergy Innovation (CBI), which is a U.S. Department of Energy Bioenergy Research Center supported by the Office of Biological and Environmental Research in the DOE Office of Science. Oak Ridge National Laboratory is managed by UT-Battelle, LLC for the US DOE under Contract Number DE-AC05-00OR22725.

Data Availability Statement

The data that supports the findings of this study are available in the supplementary material of this article.

Aaron Potkay^{1,2} 
Brandon Sloan³ 
Xue Feng^{1,2} 

¹Department of Civil Environmental, and Geo-Engineering, University of Minnesota, Twin Cities, Minneapolis, Minnesota, USA

²Saint Anthony Falls Laboratory, University of Minnesota, Twin Cities, Minneapolis, Minnesota, USA

³Environmental Sciences Division, Bioresources Science and Engineering Group, Oak Ridge National Laboratory, Oak Ridge, Tennessee, USA

References

Aparecido, L. M. T., S. Woo, C. Suazo, K. R. Hultine, and B. Blonder. 2020. “High Water Use in Desert Plants Exposed to Extreme Heat.” *Ecology Letters* 23, no. 8: 1189–1200.

Ball, J. T., I. E. Woodrow, and J. A. Berry. 1987. *A Model Predicting Stomatal Conductance and Its Contribution to the Control of Photosynthesis Under Different Environmental Conditions*. In *Progress in photosynthesis research: volume 4 proceedings of the VIIth international congress on photosynthesis* providence, Rhode Island, USA, august 10–15 (1986, 221–224. Dordrecht: Springer Netherlands.

Bassiouni, M., and G. Vico. 2021. “Parsimony vs Predictive and Functional Performance of Three Stomatal Optimization Principles in a Big-Leaf Framework.” *New Phytologist* 231, no. 2: 586–600.

Bernacchi, C. J., E. L. Singsaas, C. A. R. L. O. S. Pimentel, A. R. Portis, Jr., and S. P. Long. 2001. “Improved Temperature Response Functions for Models of Rubisco-Limited Photosynthesis.” *Plant, Cell & Environment* 24, no. 2: 253–259.

Bloomfield, K. J., I. C. Prentice, L. A. Cernusak, et al. 2019. "The Validity of Optimal Leaf Traits Modelled on Environmental Conditions." *New Phytologist* 221, no. 3: 1409–1423.

Bonan, G. B., M. Williams, R. A. Fisher, and K. W. Oleson. 2014. "Modeling Stomatal Conductance in the Earth System: Linking Leaf Water-Use Efficiency and Water Transport Along the Soil-Plant-Atmosphere Continuum." *Geoscientific Model Development* 7, no. 5: 2193–2222.

Buckley, T., J. Miller, and G. Farquhar. 2002. "The Mathematics of Linked Optimisation for Water and Nitrogen Use in a Canopy." *Silva Fennica* 36, no. 3: 639–669.

Buckley, T. N., L. Sack, and G. D. Farquhar. 2017. "Optimal Plant Water Economy." *Plant, Cell & Environment* 40, no. 6: 881–896.

Buckley, T. N., and S. J. Schymanski. 2014. "Stomatal Optimisation in Relation to Atmospheric CO₂." *New Phytologist* 201, no. 2: 372–377.

Busch, F. A., M. Holloway-Phillips, H. Stuart-Williams, and G. D. Farquhar. 2020. "Revisiting Carbon Isotope Discrimination in C3 Plants Shows Respiration Rules When Photosynthesis Is Low." *Nature Plants* 6, no. 3: 245–258.

Cernusak, L. A., G. R. Goldsmith, M. Arend, and R. T. W. Siegwolf. 2019. "Effect of Vapor Pressure Deficit on Gas Exchange in Wild-Type and Abscisic Acid-Insensitive Plants." *Plant Physiology* 181, no. 4: 1573–1586.

Cernusak, L. A., N. Ubierna, K. Winter, J. A. M. Holtum, J. D. Marshall, and G. D. Farquhar. 2013. "Environmental and Physiological Determinants of Carbon Isotope Discrimination in Terrestrial Plants." *New Phytologist* 200, no. 4: 950–965.

Cowan, I. R., and G. D. Farquhar. 1977. "Stomatal Function in Relation to Leaf Metabolism and Environment." In *Integration of Activity in the Higher Plant*, edited by D. H. Jennings, 471–505. Cambridge, UK: Cambridge University Press.

Cramer, J. S. 1987. "Mean and Variance of R₂ in Small and Moderate Samples." *Journal of Econometrics* 35, no. 2–3: 253–266.

Davidson, K. J., J. Lamour, A. McPherran, A. Rogers, and S. P. Serbin. 2023a. "Seasonal Trends in Leaf-Level Photosynthetic Capacity and Water Use Efficiency in a North American Eastern Deciduous Forest and Their Impact on Canopy-Scale Gas Exchange." *New Phytologist* 240, no. 1: 138–156.

Davidson, K. J., J. Lamour, A. Rogers, et al. 2023b. "Short-Term Variation in Leaf-Level Water Use Efficiency in a Tropical Forest." *New Phytologist* 237, no. 6: 2069–2087.

Diao, H., L. A. Cernusak, M. Saurer, A. Gessler, R. T. W. Siegwolf, and M. M. Lehmann. 2024. "Dry Inside: Progressive Unsaturation Within Leaves With Increasing Vapour Pressure Deficit Affects Estimation of Key Leaf Gas Exchange Parameters." *New Phytologist* 244: 1275–1287. <https://doi.org/10.1111/nph.20078>.

Dong, N., I. C. Prentice, I. J. Wright, et al. 2020. "Components of Leaf-Trait Variation Along Environmental Gradients." *New Phytologist* 228, no. 1: 82–94.

Drake, J. E., S. A. Power, R. A. Duursma, et al. 2017. "Stomatal and Non-Stomatal Limitations of Photosynthesis for Four Tree Species Under Drought: A Comparison of Model Formulations." *Agricultural and Forest Meteorology* 247: 454–466.

Duursma, R. A. 2015. "Plantecophys—An R Package for Analyzing and Modelling Leaf Gas Exchange Data." *PloS One* 10, no. 11: e0143346.

Duursma, R. A., C. J. Blackman, R. Lopéz, N. K. Martin-StPaul, H. Cochard, and B. E. Medlyn. 2019. "On the Minimum Leaf Conductance: Its Role in Models of Plant Water Use, and Ecological and Environmental Controls." *New Phytologist* 221, no. 2: 693–705.

Duursma, R. A., P. Payton, M. P. Bange, et al. 2013. "Near-Optimal Response of Instantaneous Transpiration Efficiency to Vapour Pressure Deficit, Temperature and [CO₂] in Cotton (*Gossypium Hirsutum L.*)." *Agricultural and Forest Meteorology* 168: 168–176.

Eller, C. B., L. Rowland, M. Mencuccini, et al. 2020. "Stomatal Optimization Based on Xylem Hydraulics (Sox) Improves Land Surface Model Simulation of Vegetation Responses to Climate." *New Phytologist* 226, no. 6: 1622–1637.

Evans, J., T. Sharkey, J. Berry, and G. Farquhar. 1986. "Carbon Isotope Discrimination Measured Concurrently With Gas Exchange to Investigate CO₂ Diffusion in Leaves of Higher Plants." *Functional Plant Biology* 13, no. 2: 281–292.

Farquhar, G. D., S. von Caemmerer, and J. A. Berry. 1980. "A Biochemical Model of Photosynthetic CO₂ Assimilation in Leaves of C 3 Species." *Planta* 149: 78–90.

Fites, J. A., and R. O. Teskey. 1988. "CO₂ and Water Vapor Exchange of *Pinus Taeda* in Relation to Stomatal Behavior: Test of an Optimization Hypothesis." *Canadian Journal of Forest Research* 18, no. 2: 150–157.

Franklin, O., S. P. Harrison, R. Dewar, et al. 2020. "Organizing Principles for Vegetation Dynamics." *Nature Plants* 6, no. 5: 444–453.

Franks, P. J., J. A. Berry, D. L. Lombardozzi, and G. B. Bonan. 2017. "Stomatal Function Across Temporal and Spatial Scales: Deep-Time Trends, Land-Atmosphere Coupling and Global Models." *Plant Physiology* 174, no. 2: 583–602.

Franks, P. J., G. B. Bonan, J. A. Berry, et al. 2018. "Comparing Optimal and Empirical Stomatal Conductance Models for Application in Earth System Models." *Global Change Biology* 24, no. 12: 5708–5723.

Gardner, A., M. Jiang, D. S. Ellsworth, et al. 2023. "Optimal Stomatal Theory Predicts CO₂ Responses of Stomatal Conductance in Both Gymnosperm and Angiosperm Trees." *New Phytologist* 237, no. 4: 1229–1241.

Gimeno, T. E., K. Y. Crous, J. Cooke, et al. 2016. "Conserved Stomatal Behaviour Under Elevated CO₂ and Varying Water Availability in a Mature Woodland." *Functional Ecology* 30, no. 5: 700–709.

Gimeno, T. E., N. Saavedra, J. Ogée, B. E. Medlyn, and L. Wingate. 2019. "A Novel Optimization Approach Incorporating Non-Stomatal Limitations Predicts Stomatal Behaviour in Species From Six Plant Functional Types." *Journal of Experimental Botany* 70, no. 5: 1639–1651.

Grieu, P., J. M. Guehl, and G. Aussenac. 1988. "The Effects of Soil and Atmospheric Drought on Photosynthesis and Stomatal Control of Gas Exchange in Three Coniferous Species." *Physiologia Plantarum* 73, no. 1: 97–104.

Grossiord, C., T. N. Buckley, L. A. Cernusak, et al. 2020. "Plant Responses to Rising Vapor Pressure Deficit." *New Phytologist* 226, no. 6: 1550–1566.

Hall, A. E., and E. D. Schulze. 1980. "Stomatal Response to Environment and a Possible Interrelation Between Stomatal Effects on Transpiration and CO₂ Assimilation." *Plant, Cell & Environment* 3, no. 6: 467–474.

Harrison, S. P., W. Cramer, O. Franklin, et al. 2021. "Eco-Evolutionary Optimality as a Means to Improve Vegetation and Land-Surface Models." *New Phytologist* 231, no. 6: 2125–2141.

Héroult, A., Y. S. Lin, A. Bourne, B. E. Medlyn, and D. S. Ellsworth. 2013. "Optimal Stomatal Conductance in Relation to Photosynthesis in Climatically Contrasting Eucalyptus Species Under Drought." *Plant, Cell & Environment* 36, no. 2: 262–274.

Holloway-Phillips, M., L. A. Cernusak, H. Stuart-Williams, N. Ubierna, and G. D. Farquhar. 2019. "Two-Source δ 18O Method to Validate the CO₂-Photosynthetic Discrimination Model: Implications for Mesophyll Conductance." *Plant Physiology* 181, no. 3: 1175–1190.

Holtzman, W. H. 1950. "The Unbiased Estimate of the Population Variance and Standard Deviation." *The American Journal of Psychology* 63, no. 4: 615–617.

Jackson, D. A., and K. M. Somers. 1991. "The Spectre of 'Spurious' Correlations." *Oecologia* 86: 147–151.

Jarvis, P. 1976. "The Interpretation of the Variations in Leaf Water Potential and Stomatal Conductance Found in Canopies in the Field." *Philosophical Transactions of the Royal Society of London. B, Biological Sciences* 273, no. 927: 593–610.

Katul, G., S. Manzoni, S. Palmroth, and R. Oren. 2010. "A Stomatal Optimization Theory to Describe the Effects of Atmospheric CO₂ on Leaf Photosynthesis and Transpiration." *Annals of Botany* 105, no. 3: 431–442.

Katul, G. G., S. Palmroth, and R. Oren. 2009. "Leaf Stomatal Responses to Vapour Pressure Deficit Under Current and CO₂-Enriched Atmosphere Explained by the Economics of Gas Exchange." *Plant, Cell & Environment* 32, no. 8: 968–979.

De Kauwe, M. G., J. Kala, Y. S. Lin, et al. 2015. "A Test of an Optimal Stomatal Conductance Scheme Within the Cable Land Surface Model." *Geoscientific Model Development* 8, no. 2: 431–452.

Knauer, J., C. Werner, and S. Zaehle. 2015. "Evaluating Stomatal Models and Their Atmospheric Drought Response in a Land Surface Scheme: A Multibiome Analysis." *Journal of Geophysical Research: Biogeosciences* 120, no. 10: 1894–1911.

Knauer, J., S. Zaehle, B. E. Medlyn, et al. 2018. "Towards Physiologically Meaningful Water-Use Efficiency Estimates From Eddy Covariance Data." *Global Change Biology* 24, no. 2: 694–710.

Lamour, J., K. J. Davidson, K. S. Ely, et al. 2022. "An Improved Representation of the Relationship Between Photosynthesis and Stomatal Conductance Leads to More Stable Estimation of Conductance Parameters and Improves the Goodness-of-Fit Across Diverse Data Sets." *Global Change Biology* 28, no. 11: 3537–3556.

Leuning, R. 1990. "Modelling Stomatal Behaviour and Photosynthesis of *Eucalyptus Grandis*." *Functional Plant Biology* 17, no. 2: 159–175.

Leuning, R. 1995. "A Critical Appraisal of a Combined Stomatal-Photosynthesis Model for C3 Plants." *Plant, Cell & Environment* 18, no. 4: 339–355.

Li, X., P. Gentine, C. Lin, et al. 2019. "A Simple and Objective Method to Partition Evapotranspiration into Transpiration and Evaporation at Eddy-Covariance Sites." *Agricultural and Forest Meteorology* 265: 171–182.

Liang, J., K. W. Krauss, J. Finnigan, H. Stuart-Williams, G. D. Farquhar, and M. C. Ball. 2023. "Linking Water Use Efficiency With Water Use Strategy From Leaves to Communities." *New Phytologist* 240, no. 5: 1735–1742.

Lin, C., P. Gentine, C. Frankenberg, S. Zhou, D. Kennedy, and X. Li. 2019. "Evaluation and Mechanism Exploration of the Diurnal Hysteresis of Ecosystem Fluxes." *Agricultural and Forest Meteorology* 278: 107642.

Lin, C., P. Gentine, Y. Huang, K. Guan, H. Kimm, and S. Zhou. 2018. "Diel Ecosystem Conductance Response to Vapor Pressure Deficit Is Suboptimal and Independent of Soil Moisture." *Agricultural and Forest Meteorology* 250–251: 24–34.

Lin, Y. S., B. E. Medlyn, R. A. Duursma, et al. 2015. "Optimal Stomatal Behaviour Around the World." *Nature Climate Change* 5, no. 5: 459–464.

Lindstrom, M. J., and D. M. Bates. 1990. "Nonlinear Mixed Effects Models for Repeated Measures Data." *Biometrics* 46: 673–687.

Liu, Y., O. Flournoy, Q. Zhang, K. A. Novick, R. D. Koster, and A. G. Konings. 2022. "Canopy Height and Climate Dryness Parsimoniously Explain Spatial Variation of Unstressed Stomatal Conductance." *Geophysical Research Letters* 49, no. 15: e2022GL099339.

Long, S. P. 2003. "Gas Exchange Measurements, What Can They Tell Us about the Underlying Limitations to Photosynthesis? Procedures and Sources of Error." *Journal of Experimental Botany* 54, no. 392: 2393–2401.

Lundberg, S. M., and S. I. Lee. 2017. "A Unified Approach to Interpreting Model Predictions." in *Proceedings of the Advances in Neural Information Processing Systems, Long Beach, CA, USA, 4–9 December 2017*, 4765–4774.

Mäkelä, A. 1996. "Optimal Control of Gas Exchange During Drought: Theoretical Analysis." *Annals of Botany* 77, no. 5: 461–468.

Manzoni, S., G. Vico, G. Katul, et al. 2011. "Optimizing Stomatal Conductance for Maximum Carbon Gain Under Water Stress: A Meta-Analysis Across Plant Functional Types and Climates." *Functional Ecology* 25, no. 3: 456–467.

Manzoni, S., G. Vico, S. Palmroth, A. Porporato, and G. Katul. 2013. "Optimization of Stomatal Conductance for Maximum Carbon Gain Under Dynamic Soil Moisture." *Advances in Water Resources* 62: 90–105.

Marchin, R. M., A. A. Broadhead, L. E. Bostic, R. R. Dunn, and W. A. Hoffmann. 2016. "Stomatal Acclimation to Vapour Pressure Deficit Doubles Transpiration of Small Tree Seedlings with Warming." *Plant, Cell & Environment* 39, no. 10: 2221–2234.

Marchin, R. M., B. E. Medlyn, M. G. Tjoelker, and D. S. Ellsworth. 2023. "Decoupling Between Stomatal Conductance and Photosynthesis Occurs Under Extreme Heat in Broadleaf Tree Species Regardless of Water Access." *Global Change Biology* 29, no. 22: 6319–6335.

Medlyn, B. E., R. A. Duursma, D. Eamus, et al. 2011. "Reconciling the Optimal and Empirical Approaches to Modelling Stomatal Conductance." *Global Change Biology* 17, no. 6: 2134–2144.

Medlyn, B. E., M. G. De Kauwe, Y. S. Lin, et al. 2017. "How Do Leaf and Ecosystem Measures of Water-Use Efficiency Compare?" *New Phytologist* 216, no. 3: 758–770.

Michaletz, S. T., M. D. Weiser, N. G. McDowell, et al. 2016. "The Energetic and Carbon Economic Origins of Leaf Thermoregulation." *Nature Plants* 2, no. 9: 16129.

Mrad, A., S. Sevanto, J. C. Domec, Y. Liu, M. Nakad, and G. Katul. 2019. "A Dynamic Optimality Principle for Water Use Strategies Explains Isohydric to Anisohydric Plant Responses to Drought." *Frontiers in Forests and Global Change* 2: 49.

Nakad, M., S. Sevanto, J. C. Domec, and G. Katul. 2023. "Linking the Water and Carbon Economies of Plants in a Drying and Warming Climate." *Current Forestry Reports* 9, no. 6: 383–400.

Novick, K. A., D. L. Ficklin, P. C. Stoy, et al. 2016. "The Increasing Importance of Atmospheric Demand for Ecosystem Water and Carbon Fluxes." *Nature Climate Change* 6, no. 11: 1023–1027.

Potkay, A., and X. Feng. 2023a. "Do Stomata Optimize Turgor-Driven Growth? A New Framework for Integrating Stomata Response With Whole-Plant Hydraulics and Carbon Balance." *New Phytologist* 238, no. 2: 506–528.

Potkay, A., and X. Feng. 2023b. "Dynamically Optimizing Stomatal Conductance for Maximum Turgor-Driven Growth over Diel and Seasonal Cycles." *AoB Plants* 15, no. 5: plad044.

Prentice, I. C., N. Dong, S. M. Gleason, V. Maire, and I. J. Wright. 2014. "Balancing the Costs of Carbon Gain and Water Transport: Testing a New Theoretical Framework for Plant Functional Ecology." *Ecology Letters* 17, no. 1: 82–91.

De Pury, D. G. G., and G. D. Farquhar. 1997. "Simple Scaling of Photosynthesis From Leaves to Canopies Without the Errors of Big-Leaf Models." *Plant, Cell & Environment* 20, no. 5: 537–557.

Raghav, P., M. Kumar, and Y. Liu. 2024. "Structural Constraints in Current Stomatal Conductance Models Preclude Accurate Prediction of Evapotranspiration." *Water Resources Research* 60, no. 8: e2024WR037652.

Rodriguez-Iturbe, I., and A. Porporato. 2004. *Ecohydrology of Water Controlled Ecosystems*, 450. New York: Cambridge University Press.

Rodriguez-Iturbe, I., A. Porporato, L. Ridolfi, V. Isham, and D. R. Cox. 1999. "Probabilistic Modelling of Water Balance at a Point: The Role of Climate, Soil and Vegetation." *Proceedings of the Royal Society of*

London. Series A: Mathematical, Physical and Engineering Sciences 455, no. 1990: 3789–3805.

Sabot, M. E. B., M. G. De Kauwe, A. J. Pitman, et al. 2022. “One Stomatal Model to Rule Them All? Toward Improved Representation of Carbon and Water Exchange in Global Models.” *Journal of Advances in Modeling Earth Systems* 14, no. 4: e2021MS002761.

Sabot, M. E. B., M. G. De Kauwe, A. J. Pitman, et al. 2020. “Plant Profit Maximization Improves Predictions of European Forest Responses to Drought.” *New Phytologist* 226, no. 6: 1638–1655.

Sloan, B. P., and X. Feng. 2023. “Robust Inference of Ecosystem Soil Water Stress From Eddy Covariance Data.” *Agricultural and Forest Meteorology* 343: 109744.

Stefanski, A., E. E. Butler, R. Bermudez, R. A. Montgomery, and P. B. Reich. 2023. “Stomatal Behaviour Moderates the Water Cost of CO₂ Acquisition for 21 Boreal and Temperate Species under Experimental Climate Change.” *Plant, Cell & Environment* 46, no. 10: 3102–3119.

Thomas, D. S., D. Eamus, and D. Bell. 1999. “Optimization Theory of Stomatal Behaviour: II. Stomatal Responses of Several Tree Species of North Australia to Changes in Light, Soil and Atmospheric Water Content and Temperature.” *Journal of Experimental Botany* 50, no. 332: 393–400.

Tuzet, A., A. Perrier, and R. Leuning. 2003. “A Coupled Model of Stomatal Conductance, Photosynthesis and Transpiration.” *Plant, Cell & Environment* 26, no. 7: 1097–1116.

Urban, J., M. W. Ingwers, M. A. McGuire, and R. O. Teskey. 2017. “Increase in Leaf Temperature Opens Stomata and Decouples Net Photosynthesis From Stomatal Conductance in *Pinus Taeda* and *Populus Deltoidea X Nigra*.” *Journal of Experimental Botany* 68, no. 7: 1757–1767.

Wang, H., I. C. Prentice, T. F. Keenan, et al. 2017. “Towards a Universal Model for Carbon Dioxide Uptake by Plants.” *Nature Plants* 3, no. 9: 734–741.

Wang, X., W. T. Ma, Y. R. Sun, et al. 2024. “The Response of Mesophyll Conductance to Short-Term CO₂ Variation Is Related to Stomatal Conductance.” *Plant, Cell & Environment* 47, no. 9: 3590–3604.

Wang, Y., and C. Frankenberg. 2022. “On the Impact of Canopy Model Complexity on Simulated Carbon, Water, and Solar-Induced Chlorophyll Fluorescence Fluxes.” *Biogeosciences* 19, no. 1: 29–45.

Wang, Y., J. S. Sperry, W. R. L. Anderegg, M. D. Venturas, and A. T. Trugman. 2020. “A Theoretical and Empirical Assessment of Stomatal Optimization Modeling.” *New Phytologist* 227, no. 2: 311–325.

Wolfe, B. T., M. Detto, Y. J. Zhang, et al. 2023. “Leaves as Bottlenecks: The Contribution of Tree Leaves to Hydraulic Resistance Within the Soil–Plant–Atmosphere Continuum.” *Plant, Cell & Environment* 46, no. 3: 736–746.

Wong, S. C., M. J. Cannan, M. Holloway-Phillips, et al. 2022. “Humidity Gradients in the Air Spaces of Leaves.” *Nature Plants* 8, no. 8: 971–978.

Yi, K., K. A. Novick, Q. Zhang, et al. 2024. “Responses of Marginal and Intrinsic Water-Use Efficiency to Changing Aridity Using Fluxnet Observations.” *Journal of Geophysical Research: Biogeosciences* 129, no. 6: e2023JG007875.

Zhai, B., G. Wang, Z. Hu, Z. Tang, and S. Sun. 2024. “Marginal Water Use Efficiencies of Different Plant Functional Types Along an Elevation Gradient in Subalpine Regions.” *European Journal of Forest Research* 143: 773–784.

Zhou, S., R. A. Duursma, B. E. Medlyn, J. W. G. Kelly, and I. C. Prentice. 2013. “How Should We Model Plant Responses to Drought? An Analysis of Stomatal and Non-Stomatal Responses to Water Stress.” *Agricultural and Forest Meteorology* 182–183: 204–214.

Zhou, S., B. Medlyn, S. Sabaté, D. Sperlich, I. C. Prentice, and D. Whitehead. 2014. “Short-Term Water Stress Impacts on Stomatal, Mesophyll and Biochemical Limitations to Photosynthesis Differ Consistently Among Tree Species From Contrasting Climates.” *Tree Physiology* 34, no. 10: 1035–1046.

Zhou, S. X., B. E. Medlyn, and I. C. Prentice. 2016. “Long-Term Water Stress Leads to Acclimation of Drought Sensitivity of Photosynthetic Capacity in Xeric but not Riparian Eucalyptus Species.” *Annals of Botany* 117, no. 1: 133–144.

Supporting Information

Additional supporting information can be found online in the Supporting Information section.